



HAL
open science

Empirical Orthogonal Functions for ecology

Baptiste Alglave, Benjamin Dufée, Said Obakrim, James T Thorson

► **To cite this version:**

Baptiste Alglave, Benjamin Dufée, Said Obakrim, James T Thorson. Empirical Orthogonal Functions for ecology. 2025. hal-04693871v2

HAL Id: hal-04693871

<https://hal.science/hal-04693871v2>

Preprint submitted on 11 Feb 2025

HAL is a multi-disciplinary open access archive for the deposit and dissemination of scientific research documents, whether they are published or not. The documents may come from teaching and research institutions in France or abroad, or from public or private research centers.

L'archive ouverte pluridisciplinaire **HAL**, est destinée au dépôt et à la diffusion de documents scientifiques de niveau recherche, publiés ou non, émanant des établissements d'enseignement et de recherche français ou étrangers, des laboratoires publics ou privés.

1 ***Journal: Ecology***

2 ***Submission Type: Statistical Report***

3 ***Title: Empirical Orthogonal Functions for Ecology***

4 Baptiste Alglave¹, Benjamin Dufée², Said Obakrim³, and James T.

5 Thorson⁴

6 **Keywords:** spatio-temporal data, dimension reduction, satellite data, NDVI,

7 species distribution model, multivariate analysis, canonical correlation

8 analysis.

1 Lab-STICC, Université Bretagne Sud, 8 rue Michel de Montaigne, 56000, Vannes, France. *Contact author:* baptiste.alglave@univ-ubs.fr

2 Laboratory of Mathematics in Bretagne Atlantique, Rue de Saint-Maudé, 56100 Vannes, France.

3 Institute of Earth Surface Dynamics, University of Lausanne, Lausanne, Switzerland.

4 Resource Ecology and Fisheries Management Division, Alaska Fisheries Science Center, National Marine Fisheries Service, NOAA, Seattle, WA 98112, USA.

Corresponding author: james.thorson@noaa.gov

9 **Abstract:** Spatio-temporal data are ubiquitous in ecology, involving large
10 spatial domains, long time periods, and multiple variables. To take
11 advantage of these data for ecological analysis, it is crucial to rely on both
12 efficient and ecologically interpretable statistical methods. Empirical
13 Orthogonal Functions (EOFs) are a widely used method for reducing the
14 dimensionality of spatio-temporal data. While EOFs are common in
15 meteorology and climate studies, their use in ecology is still emerging.

16 This paper introduces the basics of EOFs and presents new methods to
17 specifically address key ecological questions. Since EOFs lack explicit
18 ecological constraints, their results may be difficult to interpret. We propose
19 a method to rotate EOFs using a temporal ecological variable, improving
20 interpretability by better representing ecological patterns. We also explore
21 the use of EOFs in multivariate analysis to identify shared spatial and
22 temporal patterns in community and ecosystem dynamics.

23 We illustrate these methods on two case studies including NDVI satellite
24 data over France and spatio-temporal predictions from fish species
25 distribution models.

26 Our goal is to provide a clear and concise roadmap for applying EOFs to
27 ecological problems. We emphasize practical guidance through code
28 snippets and two worked examples, making the approach accessible to a
29 broad audience of ecologists.

30 **1 Introduction**

31 Spatial and temporal data are ubiquitous in ecological research. Survey data,
32 citizen-science data, satellite data or biogeochemical model outputs provide
33 huge information for unraveling ecological processes at various temporal
34 and spatial scales (Hampton et al., 2013; Grémillet, Chevallier, and Guinet,
35 2022). Given the extensive spatial and temporal coverage of all these
36 datasets, dimension reduction (or ordination) methods become critical for
37 synthesizing the information embedded within these spatio-temporal data.

38 Empirical Orthogonal Functions (EOFs) represent the keystone method for
39 performing dimension reduction on spatio-temporal data. EOFs were first
40 introduced by Lorenz (1956). Basically, they are Principal Component
41 Analysis (PCA) performed on spatio-temporal data. Since their first
42 formulation, EOFs methods have entailed a rich literature, particularly in
43 meteorology and climate applications (Hannachi, Jolliffe, and Stephenson,
44 2007). Several extensive overviews of EOFs and derived methods are
45 available in the secondary literature (Preisendorfer, 1988; Von Storch and
46 Zwiers, 2002; Cressie and Wikle, 2011; Hannachi, 2021); they mainly
47 address an audience of climatologists or statisticians.

48 Recently, these methods have expanded to ecology. They have been applied
49 to biogeochemical variables (Schrum, John, and Alekseeva, 2006; Iida and
50 Saitoh, 2007; Di Lorenzo et al., 2008; Woillez et al., 2010; Le Mezo et al.,

51 2016; Berkelhammer, 2019) as well as species distribution (Norton and
52 Mason, 2005; Petitgas, Masse, et al., 2006; Petitgas, 2008; Woillez et al.,
53 2010; Petitgas, Doray, et al., 2014; Petitgas, Huret, et al., 2018; Petitgas,
54 Renard, et al., 2020; Grandremy et al., 2023; Van Audenhaege et al., 2022).
55 EOFs have gained wider recognition through the development of the
56 Vector-Autoregressive Spatio-temporal (VAST) package (Thorson, 2019;
57 Thorson, Anderson, et al., 2024) and the application of EOFs to represent
58 the spatio-temporal variability of species communities and ecosystems
59 (Thorson, Ciannelli, and Litzow, 2020; Thorson, Cheng, et al., 2020;
60 Thorson, Arimitsu, et al., 2021). Still, these applications remain mainly
61 focused on marine systems, with very few applications to terrestrial systems
62 (Gedalof, Peterson, and Mantua, 2005; Wu et al., 2023).

63 Overall, EOFs methods can address a large range of ecological questions
64 from analyzing single species spatio-temporal variability to aiding
65 conservation decisions in an ecosystem perspectives. They allow to detect
66 seasonal signals in species distribution and shifts in phenology (Alglave,
67 Olmos, et al., 2024). Additionally, EOFs are particularly useful in tracking
68 long-term ecological changes, such as ecosystem restructuring or shifts in
69 species composition in response to climate change (Thorson, Arimitsu,
70 et al., 2021; Badger, Large, and Thorson, 2023).

71 Despite their broad potential, EOFs remain underutilized in ecology,

72 particularly in terrestrial ecosystems. In this paper, to widen EOFs
73 applications and promote their use in ecology, we provide a thorough and
74 accessible introduction to EOFs. Additionally, we describe two derived
75 methods to address specific ecological questions: (1) a method that sets
76 ecological constraints on EOFs to better disentangle the information of the
77 different dimensions of the EOFs and improve their interpretability, and (2)
78 a multivariate version of EOFs that enables to apply EOFs methodology on
79 species communities or whole ecosystems.

80 We illustrate these methods based on two real applications. First, we use a
81 terrestrial ecology example based on monthly Normalized Difference
82 Vegetation Index (NDVI) satellite data (MODIS) from 2000 to 2023
83 (MODIS, 2021). As a second case study, we use spatio-temporal predictions
84 from an Integrated Spatio-Temporal Species Distribution Model (IST-SDM)
85 (Alglave, Vermard, et al., 2023). We analyze the spatio-temporal predictions
86 spanning from 2008 to 2018 for three demersal species in the Bay of Biscay:
87 common sole (*Solea solea*, Linnaeus, 1758), squid (*Loligo vulgaris*,
88 Lamarck, 1798), and whiting (*Merlangius merlangus*, Linnaeus, 1758). In
89 the case of the IST-SDM, when the method is univariate (*i.e.* single species)
90 we focus the analysis on common sole.

91 Our goal is to provide a clear and concise roadmap for applying EOFs to
92 ecological problems. We emphasize practical guidance through code

93 snippets and two worked examples, making the approach accessible to a
94 broad audience of ecologists.

95 **2 Basics of EOFs**

96 EOFs were initially introduced by Lorenz (1956) for the analysis and
97 prediction of weather. The method involves extracting the main spatial and
98 temporal patterns that (1) capture the most variance of spatio-temporal data
99 and (2) are orthogonal to each other. In the upcoming subsections, we
100 introduce the notations and outline the principal properties of EOFs through
101 both theoretical explanations and practical applications.

102 **2.1 Continuous formulation of EOFs**

103 We denote a space-time process S such that $S(x, t)$ represents the value of
104 the process S at spatial location $x \in \mathcal{D}$ (with \mathcal{D} a continuous domain) and
105 discrete time step denoted t . When dealing with EOFs, we assume that the
106 spatio-temporal field can be decomposed into a (purely) spatial term and a
107 (purely) temporal term. In its continuous formulation, this decomposition
108 can be expressed as:

$$S(x, t) = \sum_{m=1}^{\infty} \alpha_m(t) \cdot \phi_m(x) \quad (1)$$

109 where $\phi_m(x)$ denotes the spatial term of the EOFs for dimension m and
110 $\alpha_m(t)$ represents the temporal term of the EOFs for dimension m .
111 Furthermore, $\text{var}(\alpha_1(t)) > \text{var}(\alpha_2(t)) > \dots$, and $\text{cov}(\alpha_k(t), \alpha_m(t)) = 0$,
112 for all $k \neq m$. A known solution of this problem is obtained through a
113 Karhunen-Loève expansion. Both formulation and practical estimation of
114 the EOFs in the continuous case are detailed in Cressie and Wikle (2011)
115 (p.266).

116 **2.2 Discrete formulation of EOFs**

117 The most common and straightforward way to perform EOFs on S is to
118 consider a discretized version of this process. Let's introduce the matrix \mathbf{S} of
119 size $n \times p$, where n denotes the number of discrete spatial positions, and p
120 denotes the number of time steps, with the time stepping denoted by
121 (t_1, \dots, t_p) .

122 In practice, to decompose \mathbf{S} through EOFs, these data are centered and then
123 decomposed through Singular Value Decomposition (SVD).

124 From these data, for a given spatial location x , the temporal average can be
125 calculated as:

$$\bar{S}^t(x) = \frac{1}{p} \sum_{k=1}^p S(x, t_k). \quad (2)$$

126 The time-centered space-time field, also referred to as the anomaly matrix,
 127 is then obtained by:

$$\mathbf{S}' = \mathbf{S} - \bar{\mathbf{S}}^t \mathbf{1}^\top, \quad (3)$$

128 where $\bar{\mathbf{S}}^t$ is an $n \times 1$ column vector of row means $\bar{S}^t(x)$ and $\mathbf{1}^\top$ is a $1 \times p$
 129 row vector of ones. Codes to compute the anomaly matrix are available in
 130 Supplementary Material (SM S1.1). Examples of both the raw
 131 spatio-temporal data and anomalies are available in Figure 1 for satellite
 132 NDVI data and in Figure S3.1 (SM3) for the IST-SDM case study.

133 In this case, the decomposition can be written as:

$$S'(x, t) = \sum_{m=1}^r \lambda_m \cdot u_m(x) \cdot v_m(t) \quad (4)$$

134 Here, r represents the number of dimensions of the EOFs with
 135 $r = \min(n, p)$ being the rank of the matrix \mathbf{S}' . $u_m(x)$ is a spatial term and
 136 $v_m(t)$ is a temporal term; both \mathbf{u}_m and \mathbf{v}_m have unit norm. λ_m quantifies the
 137 amplitude of the m^{th} dimension of the EOFs. The λ_m are called the singular
 138 values hereafter (see section 2.2.1).

139 The key aspect of EOFs analysis lies in the constraints imposed on the
 140 spatial terms $u_m(x)$ or the temporal terms $v_m(t)$ because they are crucial for
 141 the computation and interpretation of these indices. The most

142 straightforward and natural constraints involve (1) maximising the variance
143 explained by each spatial pattern $p_m(x)$; (2) setting orthogonal constraints
144 for both the spatial and temporal terms.

145 **2.2.1 EOFs as a solution of Singular Value Decomposition**

146 To obtain the terms $u_m(x)$ and $v_m(t)$ of equation (4), it is possible to
147 decompose \mathbf{S}' through Singular Value Decomposition (SVD), namely:

$$\mathbf{S}' = \mathbf{U}\mathbf{\Sigma}\mathbf{V}^T \quad (5)$$

148 with \mathbf{U} a $n \times r$ matrix and \mathbf{V}^T a $r \times p$ matrix, $r = \min(n, p)$ being the rank
149 of the matrix \mathbf{S}' . $\mathbf{\Sigma}$ is a $r \times r$ diagonal matrix with non-increasing positive
150 coefficients on the diagonal, denoted as $\mathbf{\Sigma} = \text{Diag}(\lambda_1, \dots, \lambda_r)$ and
151 $\lambda_1 \geq \lambda_2 \geq \dots \geq \lambda_r > 0$. This is essentially the same computation that is
152 performed when conducting PCA on any type of multivariate data.

153 The columns of $\mathbf{U} = (\mathbf{u}_1, \dots, \mathbf{u}_r)$ are referred to as the EOFs maps of the
154 anomaly matrix \mathbf{S}' . In the following, they will be referred to as **factors**; here
155 the factors are spatial. The columns of $\mathbf{V} = (\mathbf{v}_1, \dots, \mathbf{v}_r)$ contain the terms
156 $v_m(t)$ from Equation (4). They will be called **loadings**; here the loadings are
157 temporal. Finally, $\mathbf{\Sigma}$ contains the singular values of \mathbf{S}' along the diagonal.
158 Note that here, singular values cannot be related to variance because the

159 centering of \mathbf{S} is realized on rows. Codes to perform the svd are available in
160 SM1 (Section S1.2).

161 **2.2.2 Interpretation of EOFs**

162 The construction of EOFs discussed in the previous subsection implies that
163 the first EOFs map \mathbf{u}_1 is the factor that captures the most variance in \mathbf{S}' . The
164 second EOFs, \mathbf{u}_2 is the next factor that captures most variance while being
165 orthogonal to \mathbf{u}_1 . This applies to the next j^{th} factors.

166 The loadings contained in \mathbf{v}_j , where $j \in 1, \dots, r$, are temporal indices.
167 Each is associated with a corresponding factor \mathbf{u}_j . When the loading $v_j(t)$ is
168 positive, the anomaly field is distributed according to the factor \mathbf{u}_j .
169 Conversely, if $v_j(t)$ is negative, the anomaly field is distributed according to
170 $-\mathbf{u}_j$.

171 Also it is well known that identifying EOFs dimensions with specific
172 ecological (or physical) processes should be done with care (Monahan et al.,
173 2009). Indeed, because there is no explicit ecological criteria in the
174 computation of EOFs, the signal related to an ecological process could be
175 found on several dimensions. Besides, a single dimension could gather the
176 signal of different ecological processes. As so, methods derived from EOFs

177 that integrate ecological knowledge would help to better disentangle the
178 signal related to some specific ecological process.

179 Other details to interpret EOFs are provided in SM2 (*e.g.* computation of
180 the variance related to each EOFs dimension, number of dimensions to
181 retain in the analysis, whether specific dimensions can be related to physical
182 or ecological processes).

183 **3 Applying EOFs to the case studies**

184 In order to illustrate EOFs, we use two spatio-temporal datasets to serve as a
185 case study: (1) NDVI data from MODIS Vegetation Index Products (satellite
186 data on terrestrial ecosystems) and (2) spatio-temporal predictions from the
187 IST-SDM for sole in the Bay of Biscay (IST-SDM). A full description of the
188 case studies is given in SM S3.2 and S3.3. We retain the first two dimensions
189 for the NDVI case study and the first four dimensions in the IST-SDM case
190 study based on the angle identified in the scree plot (left, Figure S4.1).

191 Both satellite NDVI data as well as the IST-SDM case study emphasize
192 strong seasonality 2. In the case of the NDVI, the first and second
193 dimensions bring out seasonal cycles that can be related to temperature and
194 precipitation. For the IST-SDM, the two first dimensions highlight a signal
195 related to reproduction (onshore-offshore migration) and the second

196 dimension emphasize a signal related to northward migration. Additional
197 analysis on the EOFs results are available in SM S4.2.

198 As mentioned previously, ecological signals are mixed between the several
199 dimensions of the EOFs. For instance, both the first and second dimensions
200 for the two case studies capture similar seasonal signals (Figure 2). Also,
201 some loadings seem to mix both long term trends and seasonal trends (see
202 the second EOFs dimension of the IST-SDM case study). Disentangling the
203 ecological signals from these dimensions would benefit the ecological
204 analysis of these datasets.

205 **4 Informing EOFs with an ancillary temporal variable**

206 As mentioned in previous sections, EOFs may not effectively disentangle
207 the ecological processes that structure the data. To address this limitation,
208 informing EOFs with a temporal variable (or ancillary variable) that is
209 ecologically meaningful can improve the interpretability of EOFs patterns.

210 This section describes the methodology for extracting EOFs patterns that
211 exhibit the highest correlation with some ancillary temporal variable. This
212 process involves projecting the spatio-temporal data onto the EOFs basis
213 and then performing a Canonical correlation analysis (CCA) between a
214 selected set of EOFs loadings and the ancillary variable. We first introduce

215 the CCA method, demonstrate how to adapt it to our specific issue, and
 216 finally present applications of this technique.

217 **4.1 Basics of canonical correlation analysis**

218 CCA was first proposed by Hotelling (1992). It is a method used to identify
 219 and measure the associations among two sets of variables. Consider two
 220 space-time processes $S^{(1)}(x, t)$ and $S^{(2)}(x, t)$ at location x and time t . CCA
 221 aims at identifying pairs of spatial basis vectors, \mathbf{w}_1 and \mathbf{w}_2 , for the two
 222 processes, $S^{(1)}$ and $S^{(2)}$, that maximize the correlation between their
 223 projections onto these vectors. Consider the corresponding observed
 224 space-time matrices denoted $\mathbf{S}^{(1)}$ and $\mathbf{S}^{(2)}$ of size $n_1 \times p$ and $n_2 \times p$,
 225 respectively.

226 The CCA maximizes the following correlation coefficient ρ between
 227 $\mathbf{y}_1 = \mathbf{S}^{(1)}\mathbf{w}_1$ and $\mathbf{y}_2 = \mathbf{S}^{(2)}\mathbf{w}_2$:

$$\rho = \frac{\mathbb{E}(\mathbf{y}_1\mathbf{y}_2)}{\sqrt{\mathbb{E}(\mathbf{y}_1^2)\mathbb{E}(\mathbf{y}_2^2)}} = \frac{\mathbb{E}(\mathbf{w}_1^T\mathbf{S}^{(1)T}\mathbf{S}^{(2)}\mathbf{w}_2)}{\sqrt{\mathbb{E}(\mathbf{w}_1^T\mathbf{S}^{(1)T}\mathbf{S}^{(1)}\mathbf{w}_1)\mathbb{E}(\mathbf{w}_2^T\mathbf{S}^{(2)T}\mathbf{S}^{(2)}\mathbf{w}_2)}}. \quad (6)$$

228 Here \mathbf{y}_1 and \mathbf{y}_2 are the temporal variables that arise from the linear
 229 combination of $\mathbf{S}^{(1)}\mathbf{w}_1$ and $\mathbf{S}^{(2)}\mathbf{w}_2$ and whose correlation coefficient is to be
 230 maximised. Then, the spatial basis vectors \mathbf{w}_1 and \mathbf{w}_2 describe which areas
 231 contribute to this correlation in the dataset $\mathbf{S}^{(1)}$ and $\mathbf{S}^{(2)}$ respectively.

232 In order to find the vectors \mathbf{w}_1 and \mathbf{w}_2 that maximize ρ , we resort to the
 233 method of Lagrange multipliers, leading to a generalized eigenvalue
 234 problem (Weenink, 2003).

$$\begin{cases} (\mathbf{C}_{11}^{-1}\mathbf{C}_{12}\mathbf{C}_{22}^{-1}\mathbf{C}_{21} - \rho^2)\mathbf{w}_1 = 0 \\ (\mathbf{C}_{22}^{-1}\mathbf{C}_{21}\mathbf{C}_{11}^{-1}\mathbf{C}_{12} - \rho^2)\mathbf{w}_2 = 0 \end{cases} \quad (7)$$

235 Here, the eigenvalues ρ^2 represent the squared canonical correlations, and
 236 the eigenvectors \mathbf{w}_1 and \mathbf{w}_2 are the canonical correlation basis vectors.

237 **4.2 Coupling CCA with EOFs**

238 To inform the EOFs with a single ancillary variable, it is possible to perform
 239 a CCA on the matrix \mathbf{V} (Equation 5) composed of the loadings and an
 240 ancillary variable that we denote $An(t), t \in \{1, \dots, p\}$. Usually, to apply
 241 CCA we only retain the dimensions of the EOFs that capture the process
 242 and leave apart the remaining dimensions (see the rule of thumb in SM2). In
 243 this case, \mathbf{w}_1 are coefficients that allow to rotate the loadings as well as the
 244 related factors to obtain:

- 245 • one temporal variable that closely fit the ancillary variable. This is the
 246 combination of the EOFs loadings that maximizes the correlation
 247 with the ancillary variable.

248 • the related factor (or spatial basis vector) that is a combination of the
249 first EOFs factors. It will capture as much variance as the first pattern
250 of the EOFs but will not be orthogonal to the following EOFs.

251 Note that the two datasets $\mathbf{S}^{(1)}$ and $\mathbf{S}^{(2)}$ do not necessarily have the same
252 spatial extent, but they must have the same time stepping.

253 Such procedure will not necessarily bring out strongly different patterns
254 compared with EOFs; it will rather help to disentangle the processes
255 identified in the EOFs to ease interpretation.

256 **4.3 Illustration**

257 In this section, we inform EOFs of the NDVI satellite data with an ancillary
258 variable representing seasonality. The ancillary variable chosen here is a
259 steady seasonal signal evidencing seasonality with positive peaks in summer
260 (July) and negative peaks in winter (January - red variable in Figure 3). This
261 variable aims at disentangling the common seasonal signal shared by the
262 two first dimensions of the EOFs (Figure 2). The seasonal signal is
263 parameterized as $An(t) = A \cdot \sin(f \cdot t + D)$.

264 To have a ancillary variable that match seasonal cycles (opposite peaks in
265 January and July) we set $A = 1$ (the amplitude of the signal), $f = 1/12 \times 2\pi$
266 the frequency of the signal components and the delay component $D = 1$.

267 Note that this procedure is not invariant to a change in the phase of the
268 seasonal signal and should be fixed with care. We then perform a CCA
269 between the first two loadings of the EOFs (components of the matrix \mathbf{V} in
270 Section 2.2) and the seasonal signal. Codes to perform the analysis are
271 available in the SM section S1.3.

272 The loadings obtained from the CCA emphasize a very good fit to the
273 ancillary variable ($R^2 = 0.98$, Figure 3, top right). By comparison, the first
274 two EOFs loadings have positive, but lower correlation coefficient ($R^2 =$
275 0.82 and $R^2 = 0.57$). The spatial basis obtained through CCA displays a
276 stronger North/South gradient of NDVI compared with the two first EOFs
277 (Figure 2). NDVI are high in orange/red areas during summer (i.e. the center
278 and mountain part of France) which corresponds to high NDVI in
279 mountains and all the southern part and eastern part of France. In these
280 areas, either ice melt and temperatures become favorable for vegetation
281 growth (mountains), either temperature are high and rains remain frequent
282 which increases vegetation coverage (eastern and south western part of
283 France). In winter, these areas are colder and they can be covered by snow
284 which do not favor vegetation growth. In blue areas, NDVI is relatively
285 higher during winter. These areas have a cooler climate during winter and
286 strong precipitation which favors vegetation growth.

287 A similar analysis is performed on the IST-SDM outputs. It allows to better

288 evidence the seasonal cycle of sole reproduction and the offshore-onshore
289 gradients that shapes sole migration (Figure S4.3)

290 **5 EOFs for multivariate analysis**

291 When studying entire ecosystems or community dynamics, multiple
292 variables need to be analyzed jointly using multivariate statistical methods
293 (Ovaskainen and Abrego, 2020; Thorson, Ciannelli, and Litzow, 2020). The
294 EOFs framework is flexible and adapts to the multivariate case. It allows to
295 identify the main modes of variability across several variables and to detect
296 shared spatial patterns and temporal trends. In such cases, the underlying
297 EOFs theory remains unchanged (Section 2); only the matrix to be
298 diagonalized \mathbf{S}' is modified.

299 **5.1 Two alternatives for conducting multivariate EOFs**

300 Let $v \in \{1, \dots, s\}$ denotes the index of the different variables in the
301 analysis, and let $S^{(v)}(x, t)$ denotes the value of the space-time process for
302 location x , time t , and variable v . We denote by $\mathbf{S}^{(v)}$ the $n \times p$ matrix of the
303 spatio-temporal variable v . Two options are available when conducting
304 multivariate EOFs:

305 1. Construct the matrix by stacking the matrices row-wise. In this case,
 306 the matrix is denoted as $\mathbf{S}_{multi}^{(row)}$ with dimensions $(n \cdot s) \times p$, and it has
 307 the following structure:

$$\mathbf{S}_{multi}^{(row)} = \begin{pmatrix} \mathbf{S}^{(1)} \\ \vdots \\ \mathbf{S}^{(s)} \end{pmatrix} \quad (8)$$

308 2. Alternatively, one can construct the matrix by stacking the matrices
 309 column-wise. In this case, the matrix is denoted as $\mathbf{S}_{multi}^{(col)}$ with
 310 dimensions $n \times (p \cdot s)$ and is structured as follows:

$$\mathbf{S}_{multi}^{(col)} = \left(\mathbf{S}^{(1)} \ ; \ \dots \ ; \ \mathbf{S}^{(s)} \right) \quad (9)$$

311 Similar to standard EOFs, SVD enables to compute the factors \mathbf{U} and the
 312 loadings \mathbf{V} (Section 2). However, depending on the data stacking of the
 313 anomaly matrix, these matrices do not have the same dimensions and do not
 314 lead to the same interpretation. The first case is a **temporally synthetic**
 315 **representation** of the multivariate data. For each dimension, there is only
 316 one single time series of loadings and there are as many factors as there are
 317 variables. The loadings quantify how the different factors evolve over time.
 318 This allows to summarize the temporal variation of all the variables in one
 319 single temporal variable. A similar approach is adopted in the VAST

320 package (Thorson, 2019). The second case, is a **spatially synthetic**
321 **representation** of the data. For each dimension, there is only one factor that
322 summarizes the variability of all the variables and as many time series of
323 loadings as there are variables. The loadings of the different variables
324 quantify how these variables are related to the factor at a specific time step.

325 Note finally that in some cases, multivariate EOFs can be applied on a
326 single variable with some time-lag. In this case the different variables are
327 the lagged version of the spatio-temporal data. This typically allows for a
328 better identification of temporal patterns such as periodicity or long-term
329 trends. It is referred to as lag EOFs in this paper; it is also often referred as
330 extended EOFs in the literature (Weare and Nasstrom, 1982).

331 **5.2 Illustration**

332 To illustrate multivariate EOFs analysis, we apply the two alternative
333 approaches to the three species in the Bay of Biscay: sole, whiting, and
334 squids. These are coastal species with potentially shared spatio-temporal
335 dynamics *e.g.* same reproduction period (Alglave, Vermard, et al., 2023).

336 The temporally synthetic multivariate EOFs (EOFs on $\mathbf{S}_{multi}^{(row)}$) provides
337 seasonal loadings that represent the reproduction phenology for all the
338 species. We only retain the first two dimensions for the analysis (Figure
339 S4.1). For sole, the reproduction areas are generally consistent with those

340 identified when conducting univariate EOFs (Figure 4). For squids and
341 whittings, reproduction areas are observed along the Landes coast (45°N -
342 1.5°W), on the Vendée coast (46.5°N - 2°W), and in the north of the Bay of
343 Biscay (47.5°N - 3°W).

344 The spatially synthetic multivariate EOFs is provided in SM S4.5 as well as
345 the lag EOFs (SM S4.6). The spatially synthetic representation allows to
346 identify the common spatial patterns among each three species as well as
347 synchrony in the spatio-temporal variation of the species. The lag EOFs is
348 applied to the NDVI case study. Compared with standard EOFs (Section 3),
349 it allows to identify an additional periodic signal with a 6-months phase
350 related to an alternance of high growth of vegetation in spring and autumn
351 and lower growth in summer and winter.

352 **6 Discussion**

353 **Towards a wider use of EOFs in ecology**

354 EOFs have tremendous potential for ecology. As massive and diverse
355 datasets become available (satellite data, IST-SDM, satellite data and
356 biogeochemical models), these decomposition methods will play a growing
357 role in (1) reducing data dimensionality and (2) extracting ecologically
358 relevant and interpretable information. In this paper, we demonstrate their

359 potential for both terrestrial and marine systems. We argue that EOFs should
360 be systematically used to analyze spatio-temporal ecological datasets.

361 We presented two extensions of EOFs, one to better disentangle the
362 processes identified through EOFs and improve ecological interpretability
363 of the factor and another to apply EOFs to multivariate data. Many other
364 methods derived from EOFs could be used to perform spatio-temporal
365 analysis on ecological data and are available in the literature (Preisendorfer,
366 1988; Von Storch and Zwiers, 2002; Cressie and Wikle, 2011; Hannachi,
367 2021).

368 **Accounting for spatio-temporal correlation in EOFs**

369 One might argue that EOFs do not explicitly account for spatial or temporal
370 correlations and then are not per se a spatio-temporal method. It is true that
371 EOFs is basically a PCA representation of spatio-temporal data; the
372 spatio-temporal aspects of the method comes from the data rather than from
373 the mathematical formulation of the method per se.

374 In a spatial context, methods have been developed to better handle spatial
375 correlations and to propose multiscale decompositions of ecological data
376 (P. Legendre and L. Legendre, 2012). Specifically, ‘spatial eigenfunction
377 analysis’ (e.g., Moran’s eigenvector maps, asymmetric eigenvector maps,
378 multiscale ordination) estimate sets of eigenvectors based on spatial

379 configuration matrices. These methods could potentially be extended to
380 spatio-temporal data to identify distinct spatio-temporal scales that structure
381 ecological data.

382 More recently, Petitgas, Renard, et al. (2020) and Bez, Renard, and
383 Ahmed-Babou (2023) have proposed a method (Min-max Autocorrelation
384 Factor - MAF - or Empirical Orthogonal Maps - EOM) to provide spatially
385 decorrelated factors. EOM provide maps with stronger orthogonality
386 constraints and aims to better separate the information carried by the factors.
387 Still, such approach is very sensitive to the choice of the spatial lag chosen
388 in the analysis and does not account for temporal correlation.

389 **Non-stationary, non-linear EOFs for spatio-temporal analysis under**
390 **climate change**

391 Finally, some important hypotheses underlie EOFs, namely stationarity and
392 linearity (Hannachi, Jolliffe, and Stephenson, 2007; Alglave, Olmos, et al.,
393 2024). EOFs can not be used to describe propagating patterns such as range
394 expansion or contraction as is common in species redistribution (Melles
395 et al., 2011; Scheele et al., 2017). Also, as in standard PCA, all non-linear
396 processes will not be detected and captured through EOFs while it is largely
397 recognized that ecosystems are strongly structured by non-linear
398 relationships and sometimes switching dynamics (Scheffer et al., 2001).
399 More generally speaking, handling non-stationarity in a changing

400 environment is a key challenge for statistical ecology (Litzow et al., 2019;
401 Astigarraga et al., 2020; Bueno de Mesquita et al., 2021).

402 Although some techniques, such as Hilbert complex EOFs or non-linear
403 PCA (Esquivel and Messina, 2008; Bueso, Piles, and Camps-Valls, 2020),
404 allow to handle non-linear relationship and to evidence propagating patterns,
405 these have been scarcely used in practice to investigate the effect of climate
406 change on ecosystems. Developing and applying approaches to handle
407 non-linearity and non-stationarity is critical in analysing the effect of
408 climate change on ecosystems; it constitutes an open research avenue for
409 future study to track the effect of climate change on ecosystems.

410 **Data availability statement**

411 Codes and data are available through the link [here](#).

412 **Acknowledgments**

413 The authors are grateful to Julia Indivero (School of Aquatic and Fishery
414 Sciences, University of Washington) and Nikolai Morokhovich (School of
415 Aquatic and Fishery Sciences, University of Washington) who made the
416 internal review for the NOAA pre-submission procedure, as well as Nicolas

417 Bez who provided insightful comments on the manuscript. The findings and
418 conclusions of the present paper are those of the authors.

419 **Competing interests**

420 The authors declare that they have no conflicts of interest or competing
421 interests that could influence the content or interpretation of this manuscript.

422 **References**

- 423 Alglave, Baptiste, Maxime Olmos, et al. (2024). “Investigating fish reproduction phenology and
424 essential habitats by identifying the main spatio-temporal patterns of fish distribution”. In:
425 *ICES Journal of Marine Science*, fsae099.
- 426 Alglave, Baptiste, Youen Vermard, et al. (2023). “Identifying mature fish aggregation areas during
427 spawning season by combining catch declarations and scientific survey data”. In:
428 *Canadian Journal of Fisheries and Aquatic Sciences* 80.5, pp. 808–824.
- 429 Astigarraga, Julen et al. (2020). “Evidence of non-stationary relationships between climate and forest
430 responses: Increased sensitivity to climate change in Iberian forests”. In:
431 *Global Change Biology* 26.9, pp. 5063–5076.
- 432 Badger, JJ, SI Large, and James T Thorson (2023). “Spatio-temporal species distribution models
433 reveal dynamic indicators for ecosystem-based fisheries management”. In:
434 *ICES Journal of Marine Science* 80.7, pp. 1949–1962.
- 435 Berkelhammer, Max (2019). “Synchronous modes of terrestrial and marine productivity in the North
436 Pacific”. In: *Frontiers in Earth Science* 7, p. 73.
- 437 Bez, Nicolas, Didier Renard, and Dedah Ahmed-Babou (2023). “Empirical Orthogonal Maps (EOM)
438 and Principal Spatial Patterns: Illustration for Octopus Distribution Off Mauritania Over the
439 Period 1987–2017”. In: *Mathematical Geosciences* 55.1, pp. 113–128.
- 440 Bueno de Mesquita, Clifton P et al. (2021). “Taking climate change into account: Non-stationarity in
441 climate drivers of ecological response”. In: *Journal of Ecology* 109.3, pp. 1491–1500.
- 442 Bueso, Diego, Maria Piles, and Gustau Camps-Valls (2020). “Nonlinear PCA for spatio-temporal
443 analysis of Earth observation data”. In: *IEEE Transactions on Geoscience and Remote Sensing*
444 58.8, pp. 5752–5763.
- 445 Cressie, Noel and Christopher K Wikle (2011). *Statistics for spatio-temporal data*. John Wiley &
446 Sons.
- 447 Di Lorenzo, Emanuele et al. (2008). “North Pacific Gyre Oscillation links ocean climate and
448 ecosystem change”. In: *Geophysical research letters* 35.8.
- 449 Esquivel, P and AR Messina (2008). “Complex empirical orthogonal function analysis of wide-area
450 system dynamics”. In:
451 *2008 IEEE Power and Energy Society General Meeting-Conversion and Delivery of Electrical Energy in the 21st Century*.
452 IEEE, pp. 1–7.
- 453 Gedalof, Ze’ev, David L Peterson, and Nathan J Mantua (2005). “Atmospheric, climatic, and
454 ecological controls on extreme wildfire years in the northwestern United States”. In:
455 *Ecological Applications* 15.1, pp. 154–174.
- 456 Grandremy, Nina et al. (2023). “Hydrology and small pelagic fish drive the spatio-temporal dynamics
457 of springtime zooplankton assemblages over the Bay of Biscay continental shelf”. In:
458 *Progress in Oceanography* 210, p. 102949.

459 Grémillet, David, Damien Chevallier, and Christophe Guinet (2022). “Big data approaches to the
460 spatial ecology and conservation of marine megafauna”. In: ICES Journal of Marine Science
461 79.4, pp. 975–986.

462 Hampton, Stephanie E et al. (2013). “Big data and the future of ecology”. In:
463 Frontiers in Ecology and the Environment 11.3, pp. 156–162.

464 Hannachi, Abdelwaheb (2021). Patterns identification and data mining in weather and climate.
465 Vol. 10. Springer.

466 Hannachi, Abdelwaheb, Ian T Jolliffe, and David B Stephenson (2007). “Empirical orthogonal
467 functions and related techniques in atmospheric science: A review”. In:
468 International Journal of Climatology: A Journal of the Royal Meteorological Society 27.9,
469 pp. 1119–1152.

470 Hotelling, Harold (1992). “Relations between two sets of variates”. In:
471 Breakthroughs in statistics: methodology and distribution. Springer, pp. 162–190.

472 Iida, Takahiro and Sei-Ichi Saitoh (2007). “Temporal and spatial variability of chlorophyll
473 concentrations in the Bering Sea using empirical orthogonal function (EOF) analysis of remote
474 sensing data”. In: Deep Sea Research Part II: Topical Studies in Oceanography 54.23-26,
475 pp. 2657–2671.

476 Le Mezo, Priscilla et al. (2016). “Natural variability of marine ecosystems inferred from a coupled
477 climate to ecosystem simulation”. In: Journal of Marine Systems 153, pp. 55–66.

478 Legendre, Pierre and Louis Legendre (2012). Numerical ecology. Vol. 24. Elsevier.

479 Litzow, Michael A et al. (2019).
480 Nonstationary environmental and community relationships in the North Pacific Ocean.

481 Lorenz, Edward N (1956). Empirical orthogonal functions and statistical weather prediction. Vol. 1.
482 Massachusetts Institute of Technology, Department of Meteorology Cambridge.

483 Melles, SJ et al. (2011). “Expanding northward: influence of climate change, forest connectivity, and
484 population processes on a threatened species’ range shift”. In: Global Change Biology 17.1,
485 pp. 17–31.

486 MODIS (2021). MOD13Q1 V6. Accessed: 2024-07-11. URL:
487 <https://lpdaac.usgs.gov/products/mod13q1v006/>.

488 Monahan, A. H. et al. (2009). “Empirical Orthogonal Functions: The Medium is the Message”. In:
489 Journal of Climate 22.24, pp. 6501–6514. doi: 10.1175/2009JCLI3062.1. URL:
490 [https://journals.ametsoc.org/view/journals/clim/22/24/
491 2009jcli3062.1.xml](https://journals.ametsoc.org/view/journals/clim/22/24/2009jcli3062.1.xml).

492 Norton, JERROLD G and JANET E Mason (2005). “Relationship of California sardine (*Sardinops*
493 *sagax*) abundance to climate-scale ecological changes in the California Current system”. In:
494 California Cooperative Oceanic Fisheries Investigations Report 46, p. 83.

495 Ovaskainen, Otso and Nerea Abrego (2020).
496 Joint species distribution modelling: With applications in R. Cambridge University Press.

497 Petitgas, Pierre (2008). “Fish habitat mapping with empirical orthogonal functions”. In:
498 International Council for the Exploration of the Sea.

499 Petitgas, Pierre, Mathieu Doray, et al. (2014). “Modelling the variability in fish spatial distributions
500 over time with empirical orthogonal functions: anchovy in the Bay of Biscay”. In:
501 ICES Journal of Marine Science 71.9, pp. 2379–2389.

502 Petitgas, Pierre, Martin Huret, et al. (2018). “Ecosystem spatial structure revealed by integrated
503 survey data”. In: Progress in Oceanography 166, pp. 189–198.

504 Petitgas, Pierre, Jacques Masse, et al. (2006). “Hydro-plankton characteristics and their relationship
505 with sardine and anchovy distributions on the French shelf of the Bay of Biscay”. In:
506 Scientia Marina 70.1, pp. 161–172.

507 Petitgas, Pierre, Didier Renard, et al. (2020). “Analysing temporal variability in spatial distributions
508 using min–max autocorrelation factors: sardine eggs in the bay of biscay”. In:
509 Mathematical Geosciences 52, pp. 337–354.

510 Preisendorfer, RW (1988). Principal Component Analysis in Meteorology and Oceanography.

511 Scheele, Ben C et al. (2017). “Niche contractions in declining species: mechanisms and
512 consequences”. In: Trends in Ecology & Evolution 32.5, pp. 346–355.

513 Scheffer, Marten et al. (2001). “Catastrophic shifts in ecosystems”. In: Nature 413.6856, pp. 591–596.

- 514 Schrum, Corinna, Mike St John, and Irina Alekseeva (2006). “ECOSMO, a coupled ecosystem model
515 of the North Sea and Baltic Sea: Part II. Spatial-seasonal characteristics in the North Sea as
516 revealed by EOF analysis”. In: *Journal of Marine Systems* 61.1-2, pp. 100–113.
- 517 Thorson, James T (2019). “Guidance for decisions using the Vector Autoregressive Spatio-Temporal
518 (VAST) package in stock, ecosystem, habitat and climate assessments”. In: *Fisheries Research*
519 210, pp. 143–161.
- 520 Thorson, James T, Sean C Anderson, et al. (2024). “tinyVAST: R package with an expressive
521 interface to specify lagged and simultaneous effects in multivariate spatio-temporal models”. In:
522 *arXiv preprint arXiv:2401.10193*.
- 523 Thorson, James T, Mayumi L Arimitsu, et al. (2021). “Forecasting community reassembly using
524 climate-linked spatio-temporal ecosystem models”. In: *Ecography* 44.4, pp. 612–625.
- 525 Thorson, James T, Wei Cheng, et al. (2020). “Empirical orthogonal function regression: Linking
526 population biology to spatial varying environmental conditions using climate projections”. In:
527 *Global Change Biology* 26.8, pp. 4638–4649.
- 528 Thorson, James T, Lorenzo Ciannelli, and Michael A Litzow (2020). “Defining indices of ecosystem
529 variability using biological samples of fish communities: a generalization of empirical
530 orthogonal functions”. In: *Progress in Oceanography* 181, p. 102244.
- 531 Van Audenhaege, Loic et al. (2022). “Long-term monitoring reveals unprecedented stability of a vent
532 mussel assemblage on the Mid-Atlantic Ridge”. In: *Progress in Oceanography* 204, p. 102791.
- 533 Von Storch, Hans and Francis W Zwiers (2002). *Statistical analysis in climate research*. Cambridge
534 university press.
- 535 Weare, Bryan C and John S Nasstrom (1982). “Examples of extended empirical orthogonal function
536 analyses”. In: *Monthly Weather Review* 110.6, pp. 481–485.
- 537 Weenink, David (2003). “Canonical correlation analysis”. In:
538 *Proceedings of the Institute of Phonetic Sciences of the University of Amsterdam*. Vol. 25.
539 University of Amsterdam Amsterdam, pp. 81–99.
- 540 Wouillez, Mathieu et al. (2010). “Statistical monitoring of spatial patterns of environmental indices for
541 integrated ecosystem assessment: Application to the Bay of Biscay pelagic zone”. In:
542 *Progress in Oceanography* 87.1-4, pp. 83–93.
- 543 Wu, Qiong et al. (2023). “Spatiotemporal variations of water conservation function based on EOF
544 analysis at multi time scales under different ecosystems of Heihe River Basin”. In:
545 *Journal of Environmental Management* 325, p. 116532.

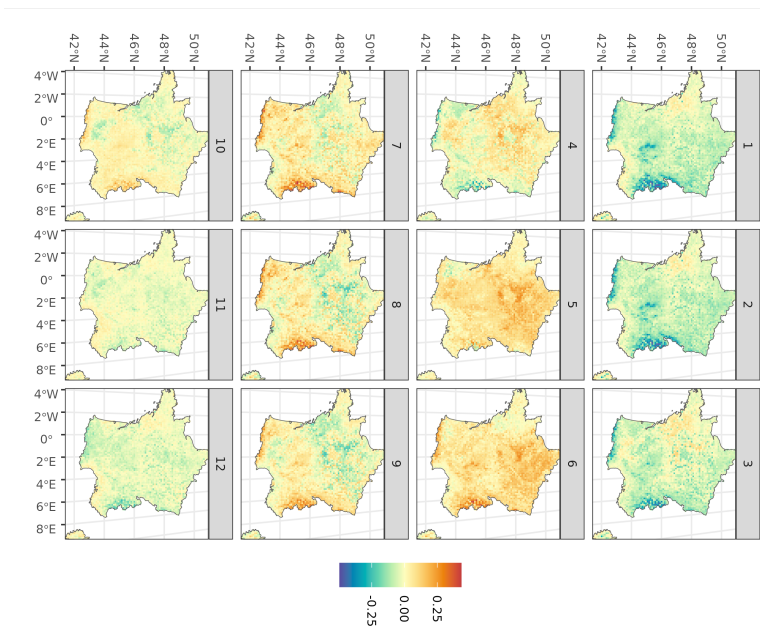
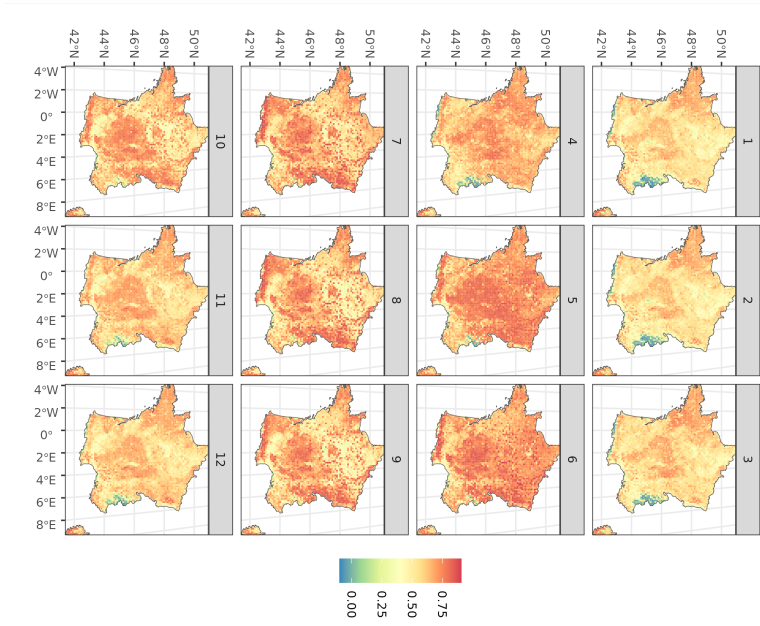


Fig. 1: NDVI data. (left) Monthly spatial data of NDVI $S(x, t)$. (right) Monthly anomalies of the spatial predictions $S^*(x, t)$. Each panel corresponds to the average predictions or anomalies for a month over the period 2000 - 2023.

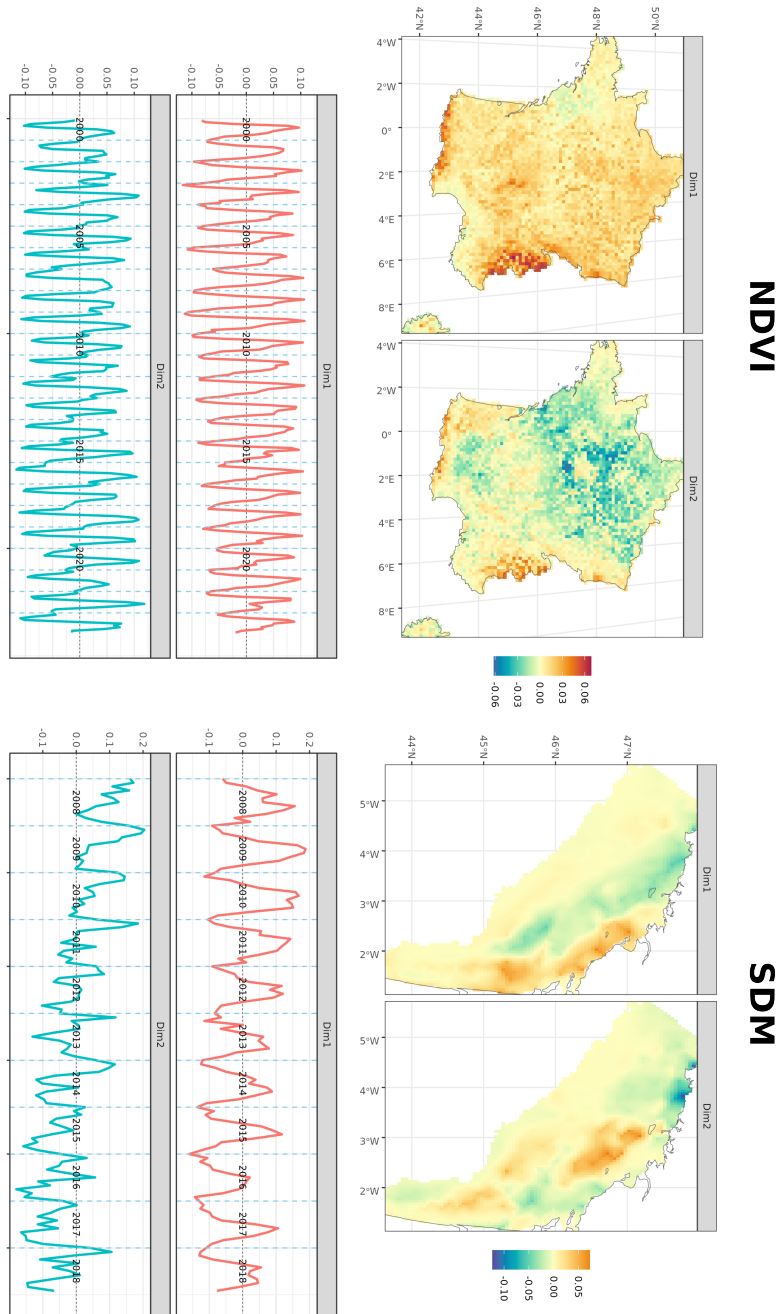


Fig. 2: EOFs results for satellite NDVI data (left) and IST-SDM predictions (right). (Top) Factors for the two first dimensions of the EOFs. (Bottom) Loadings for the two first dimensions of the EOFs. Blue dashed vertical lines correspond to the month of January for each year. The third and fourth dimensions of the IST-SDM case study are presented in Figure S4.2.

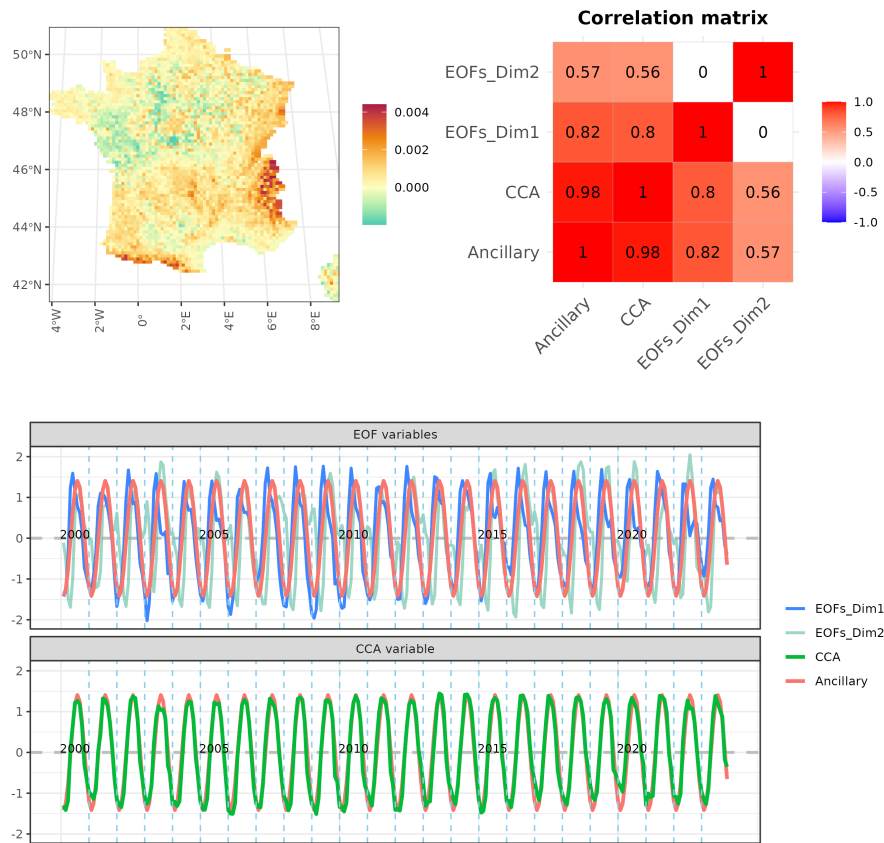


Fig. 3: Satellite NDVI data. Results of the canonical correlation analysis. (Top left) Spatial basis vector that maximizes the correlation between the temporal variables y_1 and y_2 . (Top right) Correlation matrix between the two first EOFs loadings, the CCA y_1 , and the ancillary variable. (Bottom) Comparison of the EOFs loadings with the ecological ancillary variable, and the CCA variable with the ecological ancillary variable. These time series are standardized. Blue dashed vertical lines correspond to the month of January for each year.

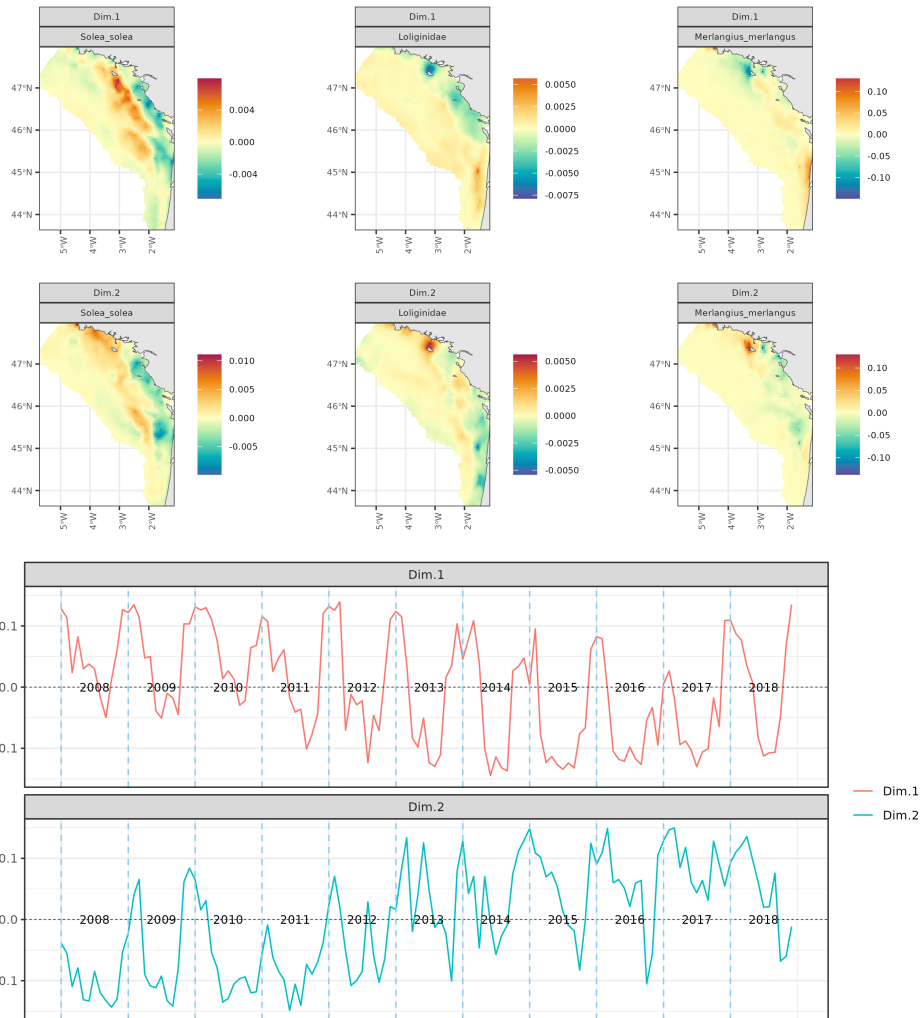


Fig. 4: IST-SDM predictions. Results for the multivariate temporally synthetic EOFs (EOFs on $\mathbf{S}_{multi}^{(row)}$). (Top) Factor maps for each species and first two dimensions. (Bottom) Loadings for the first two dimensions. Blue dashed vertical lines correspond to the month of January for each year. The loadings emphasize the seasonality of the reproduction for each three species. Orange areas in both dimensions correspond to the reproduction grounds.